References

Chamani, M. R., and Rajaratnam, N. (1994). "Jet flow on stepped spillways." *J. Hydraul. Eng.*, 120(2), 254–259.

Discussion of "Energy Dissipation and Turbulent Production in Weak Hydraulic Jumps" by E. Mignot and R. Cienfuegos

February 2010, Vol. 136, No. 2, pp. 116–121.
DOI: 10.1061/(ASCE)HY.1943-7900.0000124

Martín Romagnoli[1]; Carlos M. García[2]; and Raúl A. Lopardo[3]

[1]Research Assistant, CURIHAM, Univ. Nacional de Rosario, Riobamba 245 bis, Rosario, Santa Fe, Argentina. E-mail: martinromagnoli@gmail.com

[2]Professor, Laboratorio de Hidráulica de la Univ. Nacional de Córdoba, Av. Filloy s/n Ciudad Universitaria, Córdoba, Argentina (corresponding author). E-mail: cgarcia2mjc@gmail.com

[3]Director, Instituto Nacional del Agua, AU Ezeiza Cañuelas Tramo Jorge Newbery—km 1,620, Ezeiza, Buenos Aires, Argentina. E-mail: rlopardo@ina.gov.ar

The authors reported experimental results on the spatial evolution of turbulent kinetic energy and turbulence production in free weak hydraulic jumps. They performed turbulence measurements using two different 16 MHz SonTek/YSI microacoustic Doppler velocimeters (ADVs) on hydraulic jumps for inflow Froude numbers (F_1) of 1.3, 1.9, and 2 [$F_1 = U_1/(z_1 g)^{0.5}$, where U_1 = inflow mean velocity; z_1 = supercritical depth; and g = gravitational acceleration]. Herein the discussers aim to complement the authors' analysis by using a new independent data set and by arguing both the bias on the estimated values of turbulent kinetic energy because of the effects of the ADV sampling strategy and the uncertainty on the experimental determination of the turbulence production term.

The independent data set analyzed in this discussion has been recorded on free hydraulic jumps produced in a rectangular flume 0.65 m wide, 1.00 m deep and 12.00 m long (see experimental conditions listed in Table 1). Water velocity time signals were recorded by using an instrument similar to the one the authors used: a microacoustic Doppler velocimeter (microADV SonTek/YSI 16 MHz) with a down-looking configuration. Vertical profiles of water velocity time signals were recorded in the flume centerline at different locations within the jumps with vertical distance intervals of 0.01 m. The minimum distance from the bottom boundary to where velocity measurements are reported in this discussion is 0.02 m to avoid boundary effects (Liu et al. 2002; Precht et al. 2006; Chanson et al. 2007). The selected length of the recorded water velocity signals was 8,192 samples at 50 Hz sampling frequency. The sampling time was approximately 500 times the largest turbulence time scale expected to be present in the model.

Table 1. Experimental Conditions

Test	z_1 (m)	U_1 (m/s)	F_1	z_2 (m)	Q (L/s)	R_1
1	0.045	1.68	2.5	0.139	49.02	7.52×10^4
2	0.045	1.41	2.1	0.120	40.92	6.30×10^4

Note: undeveloped inflow; z_1 and z_2 = supercritical and subcritical depths, respectively; U_1 = inflow mean velocity; F_1 = inflow Froude number $F_1 = U_1/(z_1 g)^{0.5}$; g = gravitational acceleration; Q = flow discharge; R_1 = inflow Reynolds number $R_1 = U_1 z_1/\nu$; and ν = kinematic water viscosity.

Effects of the ADV Sampling Strategy on the Estimation of Turbulent Kinetic Energy

ADVs are capable of reporting a good description of flow turbulence when certain conditions are satisfied (Voulgaris and Trowbrigde 1998; García et al. 2005). Chanson et al. (2007) claim that raw ADV velocity data are not true turbulence and should never be used without adequate postprocessing. Throughout the measurements, aeration effects and high turbulent intensities present in free hydraulic jumps might cause spikes in the water velocity signals recorded using ADVs. These spikes must be detected and removed (Wahl 2003). Additionally, Doppler noise constitutes an important error source in acoustic Doppler measurements, and its effects on the turbulence parameters, computed from these signals, must be quantified and removed in certain cases (García et al. 2005).

Finally, ADVs produce a reduction in all of the even moments in the water velocity signal because of the sampling strategy used by this velocimetry technique (García et al. 2005). The authors performed corrections on issues related to both the presence of spikes and Doppler noise. However, no analysis has been included in the paper on the effect of the ADV sampling strategy on the estimation of turbulence parameters (i.e., turbulent kinetic energy). This issue is analyzed in this discussion on the basis of the new independent data set. In addition, the discussion explores the relative contribution of each error source in acoustic Doppler measurements in free hydraulic jumps (i.e., presence of spikes, Doppler noise, and filtering effects because of the ADV sampling strategy) on the evaluation of turbulent kinetic energy values.

The presence of spikes in the signal was detected by means of the phase-space thresholding method (PSTM) proposed by Goring and Nikora (2002) as modified in Wahl (2003). The replacement was computed by interpolation with a third-order polynomial fitted using 12 points on either side of the spike (Goring and Nikora 2002). After that, mean flow velocity values and power spectra were computed for each flow velocity component. Empirical Doppler noise energy levels were obtained by averaging the energy levels in the tail end of the power spectra within 1 Hz of the frequency range (Voulgaris and Trowbridge 1998). Corrected power spectra of the Doppler noise were then obtained by subtracting the identified noise energy level from the original power spectra for each flow velocity component. Thus, the corrected variance subtracting the Doppler noise effect was estimated for each flow velocity component as the integral of the corrected power spectra. The influence of the ADV sampling strategy on the corrected variance was analyzed to quantify digital filtering effects (García et al. 2005). The main parameter used in this analysis is $F_s = f_R L/U_c$, where f_R = sampling frequency; L = energy-containing eddy length scale; and U_c = convective velocity. The parameter F_s was estimated assuming L equal to the water depth and U_c as the local value of the mean velocity in the longitudinal direction. Once a parameter F_s has been calculated, the variance for each velocity component is corrected by filtering effects using the ADV performance curves (APCs) presented by García et al. (2005). In consequence, the turbulent kinetic energy values corrected by both Doppler noise and filtering effects have been calculated as $k = (u'^2 + v'^2 + w'^2)/2$, where u'^2, v'^2, and w'^2 = corrected variances for the longitudinal, transversal, and vertical directions, respectively.

Fig. 1 displays the spatial evolution of vertical averaged relative error of turbulent kinetic energy k produced by each error source (i.e., presence of spikes, Doppler noise, and filtering effects because of the ADV sampling strategy) with x/z_1 (x = longitudinal distance from the starting point of the jump) for F_1 of 2.1 and 2.5. In general, vertical averaged relative errors produced by presence

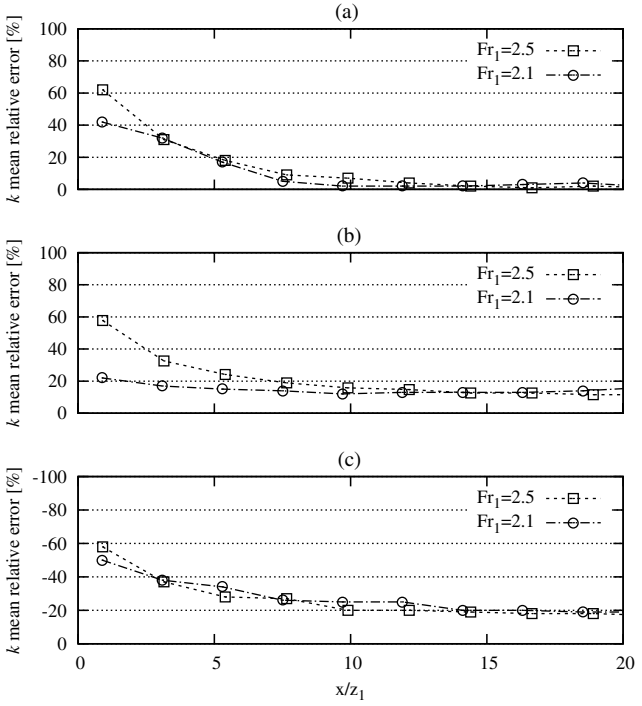

Fig. 1. Spatial evolution of vertical averaged relative error of turbulent kinetic energy k, produced by each error source: (a) presence of spikes; (b) Doppler noise; (c) filtering effects; dashed line with squares $F_1 = 2.5$, dash-dotted line with circles $F_1 = 2.1$

of spikes, Doppler noise, and filtering effects decrease along downstream direction. Furthermore, vertical averaged relative error caused by the Doppler noise decreases as F_1 decreases [Fig. 1(b)]. On the other hand, negatives values indicate underestimation in the computation of k because of ADV digital filtering effects [Fig. 1(c)]. On the basis of the new independent data set, the vertical averaged relative error of k produced by filtering effects ranges from 20–60%. Thus, it should be emphasized that the values of k reported by the authors could be biased low because of filtering effects, and the underestimation would range from 20–60%.

Uncertainty in the Experimental Determination of the Turbulence Production Term

An uncertainty analysis on the experimental determination of turbulence parameters (i.e., mean velocity, turbulent kinetic energy, shear stress, and turbulent kinetic energy dissipation and production) is required for analyzing the spatial evolution of this parameter and comparing the reported data with results from other laboratory or numerical experiments. The error involved in the experimental determination of a turbulence parameter presents several components: errors because of the experimental setup (i.e., misallocation of the instrument); errors because of the physical constraint of the measurement technique (i.e., size of the sampling volume and sampling frequency of the instrument); statistical errors because of sampling a random signal, and errors because of the methodology used to compute the parameters (e.g., scaling relations provide only orders of magnitude of the parameter) (Garcia et al. 2006). This discussion focuses on the uncertainty analysis quantifying the statistical errors of the turbulence production term and the turbulence parameters involved in its estimation on the basis of the new data set.

These statistical errors generate scatter in repeated measurement of parameters when the same experimental setup, instrument, and methodology are used. The estimation of this error component defines an estimate of the lower bound of the total error and provides a good estimate of the total error when the others errors components are minimized and relatively small compared to the sampling error (Garcia et al. 2006).

To estimate the statistical error on the experimental determination of the turbulence production term, first an estimate of the 90% confidence intervals for both U and $< uw >$ in each sampling location was computed by using the moving block boostrap (MBB) technique. MBB was shown by García et al. (2006) to provide a

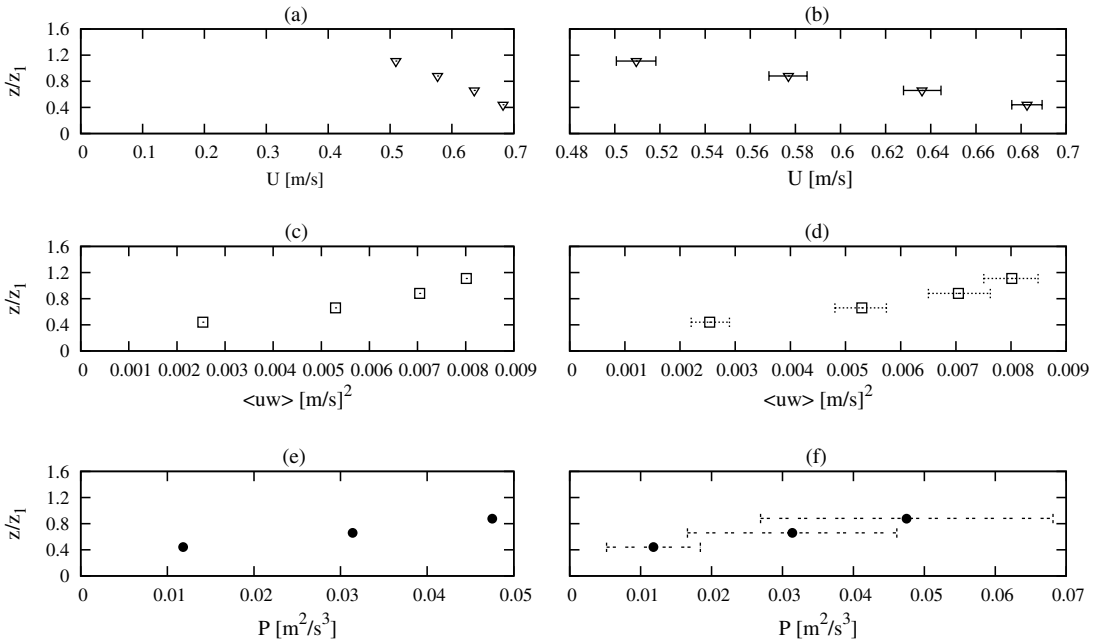

Fig. 2. Vertical profiles of time-averaged longitudinal velocity U (m/s), Reynolds shear stress $< uw > (\mathrm{m/s})^2$ and turbulence production term $P = - < uw > \partial U/\partial z$ $(\mathrm{m^2/s^3})$ for inflow F_1 = 2.1 and x/z_1 = 7.6; plots on the right include the 90% confidence intervals

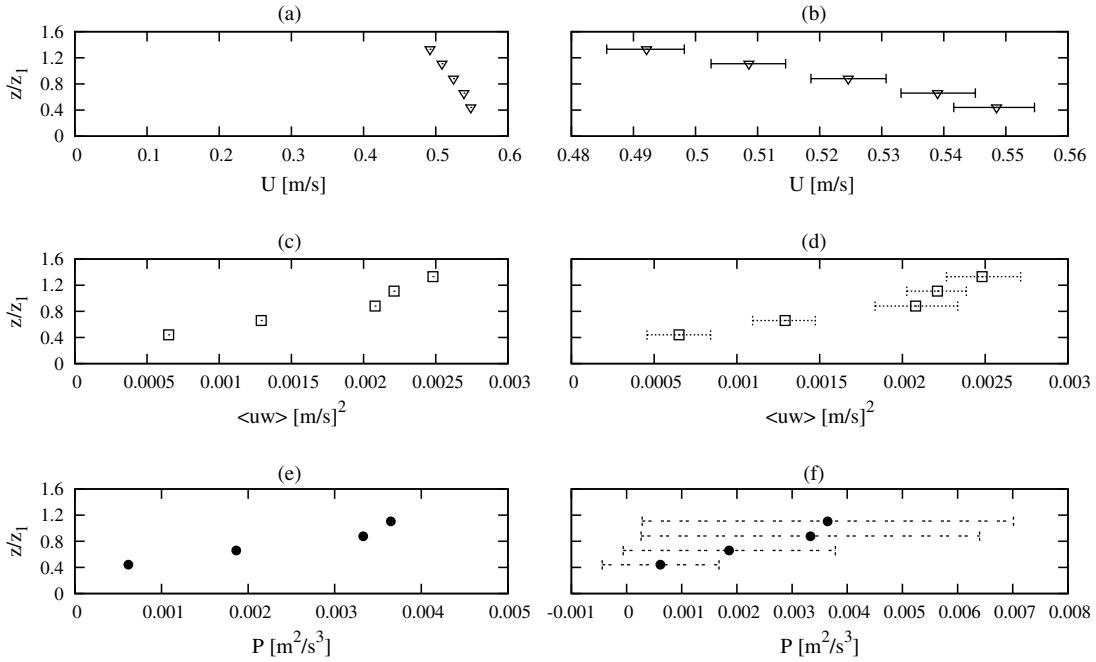

Fig. 3. Vertical profiles of time-averaged longitudinal velocity U (m/s), Reynolds shear stress $< uw >$ $(\mathrm{m/s})^2$ and turbulence production term $P = - < uw > \partial U/\partial z$ $(\mathrm{m^2/s^3})$ for inflow F_1 = 2.1 and x/z_1 = 16.5; plots on the right include the 90% confidence intervals

good approximation of the statistical error generated during the characterization of turbulence parameters. A key parameter in the MBB technique is the optimum length of the block. The optimum block length considered here was estimated by using the methodology proposed by Politis and White (2004) based on the observed autocorrelation function of each recorded signal (García et al. 2006).

The turbulence production term has been quantified at each sampling location by the authors from Reynolds shear stress locally estimated and time-averaged longitudinal velocity profiles as $P = - < uw > \partial U/\partial z$. Once the confidence intervals for both U and $< uw >$ were estimated, error propagation was computed assuming all errors are independent and using the usual formula for error propagation (Taylor 1997):

$$\sigma_P^2 = (\partial P/\partial < uw >)^2 \sigma_{<uw>}^2 + [\partial P/\partial(\Delta U)]^2 \sigma_{(\Delta U)}^2 + [\partial P/\partial(\Delta z)]^2 \sigma_{(\Delta z)}^2 \quad (1)$$

where σ_j = standard deviation error for the j magnitude and $\partial U/\partial z \approx \Delta U/\Delta z$. Thus

$$\sigma_P^2 = (-\Delta U/\Delta z)^2 \sigma_{<uw>}^2 + (- < uw > /\Delta z)^2 \sigma_{(\Delta U)}^2 + (< uw > \Delta U/\Delta z^2)^2 \sigma_{(\Delta z)}^2 \quad (2)$$

Whether or not the errors are independent, the following Schwarz inequality implies the upper bound (Taylor 1997):

$$\sigma_P \leq | - \Delta U/\Delta z| \sigma_{<uw>} + |(- < uw > /\Delta z)| \sigma_{(\Delta U)} + |(< uw > \Delta U/\Delta z^2)| \sigma_{(\Delta z)} \quad (3)$$

Once σ_P is estimated by using Eqs. (2) and (3), the interval around the measured value of the P within which the true value is expected to lie (called the confidence interval) can be computed assuming a normal probability distribution of the parameter, which generates a symmetric interval around the mean value of the parameters as $P \pm Z^{(1-\alpha)} \sigma_p$, where $Z^{(1-\alpha)} = 1.645$ for $\alpha = 0.05$. The coverage property of this interval implies that $100(1 - 2\alpha)\%$ of the time, the interval $P - Z^{(1-\alpha)} \sigma_p < P < P + Z^{(1-\alpha)} \sigma_p$ will constrain the true value of P.

Figs. 2 and 3 show vertical profiles of U, $< uw >$, and the turbulence production term $P = - < uw > \partial U/\partial z$, including the 90% confidence intervals, for inflow F_1 of 2.1 and x/z_1 of 7.6 and 16.5, respectively. $\sigma_{(z)} = 0.001$ m has been used in this analysis.

The length of the confidence intervals of U [Figs. 2(b) and 3(b)] are lower than 3% of the measured value. On the other hand, the confidence intervals length of $< uw >$ [Figs. 2(d) and 3(d)] range from 15–60% of the measured value. Using this information, the confidence intervals length of P, according to Eqs. (2) and (3), range from 40–195% and 85–340% [Figs. 2(f) and 3(f)] of the computed value, respectively. The length of the confidence interval of P precludes a precise analysis of the spatial evolution of this parameter and should be noted when comparing the reported data with results from other laboratory or numerical experiments.

References

Chanson, H., Trevethan, M., and Koch, C. (2007). "Discussion of 'Turbulence measurements with acoustic Doppler velocimeters' by Carlos M. García, Mariano I. Cantero, Yarko Niño, and Marcelo H. García." *J. Hydraul. Eng.*, 133(11), 1283–1286.

García, C. M., Cantero, M., Niño, Y., and García, M. (2005). "Turbulence measurements with acoustic Doppler velocimeters." *J. Hydraul. Eng.*, 131(12), 1062–1073.

García, C., Jackson, P., and García, M. (2006). "Confidence intervals in the determination of turbulence parameter." *Exp. Fluids*, 40, 514–522.

Goring, D., and Nikora, V. (2002). "Despiking acoustic Doppler velocimeter data." *J. Hydraul. Eng.*, 128(1), 117–126.

Liu, M., Zhu, D. Z., and Rajaratnam, N. (2002). "Evaluation of ADV measurements in bubbly two-phase flows." *Proc., Hydraulic Measurements and Experimental Methods Conf.*, ASCE, Reston, VA, 57.

Politis, D., and White, H. (2004). "Automatic block-length selection for the dependant bootstrap." *Econometric Rev.*, 23, 53–70.

Precht, E., Janssen, F., and Huettel, M. (2006). "Near-bottom performance of the acoustic Doppler velocimeter (ADV)—A comparative study." *Aquat. Ecol.*, 40, 481–492.

Taylor, J. R. (1997). *An introduction to error analysis: The study of uncertainties in physical measurements*, 2nd Ed., University Science Books, Sausalito, CA.

Voulgaris, G., and Trowbridge, J. (1998). "Evaluation of the acoustic Doppler velocimeter (ADV) for turbulence measurements." *J. Atmos. Ocean. Technol.*, 15, 272–288.

Wahl, T. L. (2003). "Discussion of 'Despiking acoustic Doppler velocimeter data' by D. Goring and V. Nikora." *J. Hydraul. Eng.*, 129(6), 484–487.

Discussion of "Energy Dissipation and Turbulent Production in Weak Hydraulic Jumps" by E. Mignot and R. Cienfuegos

February 2010, Vol. 136, No. 2, pp. 116–121.
DOI: 10.1061/(ASCE)HY.1943-7900.0000124

Iwao Ohtsu, M.ASCE[1]; Youichi Yasuda, M.ASCE[2]; and Masayuki Takahashi, A.M.ASCE[3]

[1]Professor, Dept. of Civil Engineering, Nihon Univ., College of Science and Technology, Kanda-Surugadai 1-8, Chiyoda-ku, Tokyo, 101-8308, Japan.

[2]Professor, Dept. of Civil Engineering, Nihon Univ., College of Science and Technology, Kanda-Surugadai 1-8, Chiyoda-ku, Tokyo, 101-8308, Japan.

[3]Assistant Professor, Dept. of Civil Engineering, Nihon Univ., College of Science and Technology, Kanda-Surugadai 1-8, Chiyoda-ku, Tokyo, 101-8308, Japan (corresponding author). E-mail: masayuki@civil.cst.nihon-u.ac.jp

The authors study the energy dissipation and the turbulence production in hydraulic jumps of low inflow Froude number. The discussers would like to show the hydraulic conditions required to form several types of jumps in a low Froude number range ($1.3 \le F_1 \le 3.5$). Also, the discussers would like to comment on the energy dissipation in jumps and the length of jumps.

Flow Conditions of Hydraulic Jumps

Recently, the authors, Lennon and Hill (2006), Liu et al. (2004), and Svendsen et al. (2000) investigated the velocity and turbulence characteristics in jumps for low Froude numbers. However, the flow conditions have not been shown clearly in their experiments. It is important to know the flow conditions of jumps because the flow conditions influence the velocity and turbulence characteristics of jumps. In a low Froude number range, the flow conditions of jumps below a sluice gate depend not only on the inflow Froude number F_1, but also on the Reynolds number R, the aspect ratio ℓ/h_1, and the state of boundary layer development of the supercritical inflow (Ohtsu et al. 2002, 2003, 2009). For jumps with a fully developed inflow [Fig. 1(a)], the flow conditions have been classified into three types for $\ell/h_1 \ge 10$ (nonbreaking undular jump, breaking undular jump, and classical jump) (Ohtsu et al. 2003), as shown in Fig. 2. For jumps with the inflow at the vena contracta section [Fig. 1(b)], the flow conditions have been classified into two types for $R \ge 6.0 \times 10^4$ (breaking undular jump and classical jump), as shown in Fig. 3 (Ohtsu et al. 2002). In Figs. 2 and 3, the data by the authors, Ohtsu et al. (2002, 2003, 2009), Lennon and Hill (2006), Liu et al. (2004), and Svendsen et al. (2000) are included, and each flow condition might correspond to the jump type classified by the discussers.

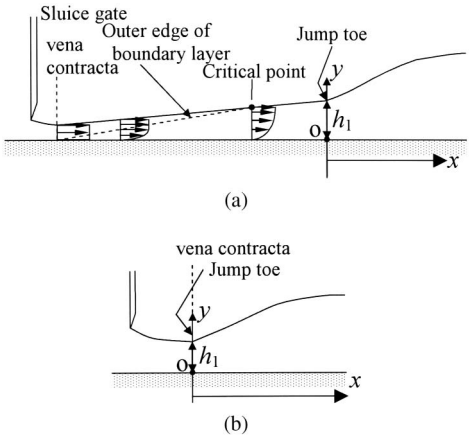

Fig. 1. Definition sketch: (a) fully developed inflow condition; (b) inflow at vena contracta section

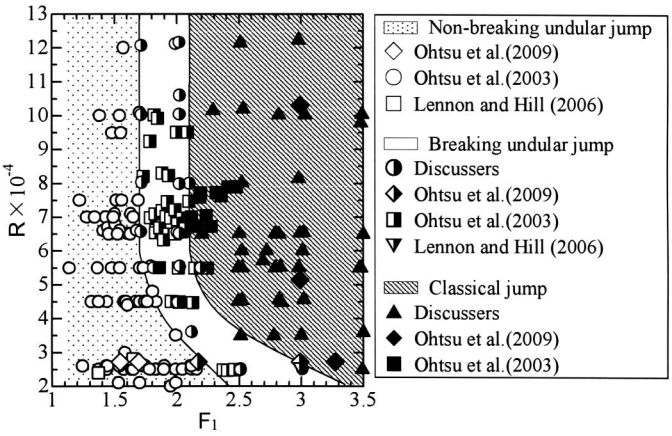

Fig. 2. Formation of jumps with fully developed inflow ($\ell/h_1 \ge 10$)

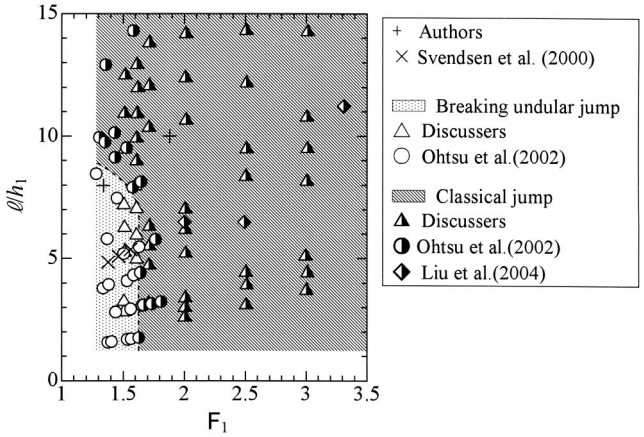

Fig. 3. Formation of jumps with inflow at vena contracta section ($R \ge 6.0 \times 10^4$)

Energy Dissipation and Length of Jump

The authors intended to clarify the characteristics of the energy dissipation and the turbulent production in hydraulic jumps of low